JOURNAL OF SOLID STATE CHEMISTRY 19, 193–204 (1976)

Optical and Structural Investigation of the Lanthanum β-Alumina Phase Doped with Europium

J. DEXPERT-GHYS, M. FAUCHER, AND P. CARO

Laboratoire des Terres Rares CNRS, 1, Place A. Briand, 92190-Meudon, France

Received January 14, 1976; in revised form May 29, 1976

The lanthanum β-alumina phase doped with europium was investigated by X-ray diffraction and fluorescence. This nonstoichiometric phase exists over the composition range: $11Al_2O_3/1La_2O_3$ to $14Al_2O_3/1La_2O_3$. The unit cell is hexagonal with $a = 5.560 \pm 0.003$ Å, $c = 22.001 \pm 0.003$ Å and belongs to the $P6_3/mmc$ space group. X-ray diffraction patterns do not vary between both boundary compositions, but fluorescence spectra show that the structure of the mirror plane in which the lanthanide ions are located is deeply modified. The atomic structure of the mirror plane is of "β-type" (like β(Na) or β(Ag)) for the lower alumina contents; it gradually changes to a "magnetoplumbite type" for higher alumina contents.

Introduction

A β-alumina type phase was first identified by Roth *et al.* in 1958 in the system Al_2O_3/La_2O_3 (*1*). Rollin *et al.* (*2*) established a phase diagram for this system and Goldberg (*3*) established diagrams for the systems Al_2O_3/Ln_2O_3 (Ln = Nd, Sm). They checked the existence of a noncongruent-melting-point compound between the corundum α-Al_2O_3 and the perovskite $LnAlO_3$(P), of approximate composition 10–$11Al_2O_3/1Ln_2O_3$. We have undertaken the structural analysis of this phase, denoted hereafter by β(La), by X-ray diffraction and spectroscopy using europium substituted for lanthanum.

We shall describe the structure of β(La) by comparing it with $BaAl_{12}O_{19}$ (isomorphous with $PbFe_{12}O_{19}$ and $BaFe_{12}O_{19}$, both of which exhibit the magnetoplumbite structure) and with β-alumina (Na): $NaAl_{11}O_{17}$ These compounds also may be written as: $[Al_{11}O_{16}]^+$ $[BaAlO_3]^-$ and $[Al_{11}O_{16}]^+[NaO]^-$. The atomic arrangement of the blocks with a spinel structure $[Al_{11}O_{16}]^+$ is practically the same in both cases (*4*, *5*). On the contrary, the mirror planes (at $z = 0.25$ and 0.75 in the hexagonal unit cell) are differently occupied. The ion positions, perfectly defined for magnetoplumbite, are shown in Fig. 1: Ba (2*d*), Al (2*b*), O (6*h*) ($x = 0.186$). In β(M) the position of the oxygen ions is in or near (2*c*), but the M^+ are differently located according to the nature of the metal ion Na^+ (*6*) or Ag^+ (*7*). The partial occupancy of the mirror plane allows for a great mobility of the metal ions which explains the high conductivity of the β-aluminas of monovalent ions.

In the case of the β(La) phase we assume that the spinel blocks remain unchanged. Our problem consists of determining the atomic composition and arrangement in the mirror plane taking into account the trivalent character of the cation $Ln^{3+} = La^{3+} + Eu^{3+}$. We mainly used two complementary methods of investigation: X-ray diffraction and optical spectroscopy. The first enables us to determine the position of the heavy atoms Ln^{3+} and gives information about the position of the light atoms. The second is sensitive to the point site symmetry of the lanthanide ion and enables us, in the present case, to locate the anions with respect to Ln^{3+}. The Eu^{3+} ion, which is optically active, is partially substituted for lan-

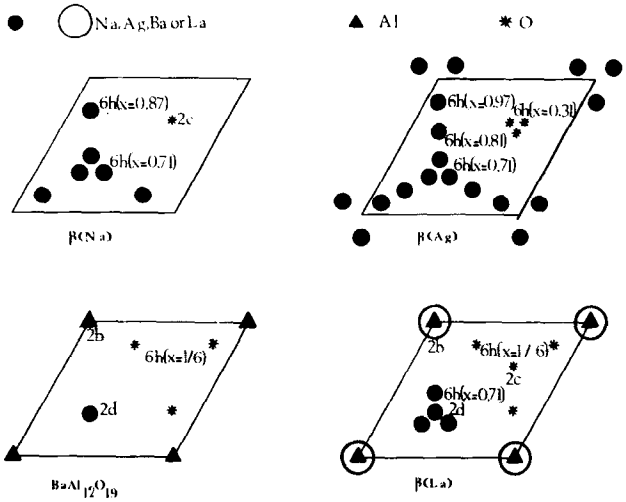

FIG. 1. Structure in the mirror plane ($z = \frac{1}{4}$) for β(Na), β(Ag), $BaAl_{12}O_{19}$, and β(La). Space group, $P6_3/mmc$.

thanum as a local structural probe, since the fluorescence spectrum of this ion is characteristic of its coordination polyhedron. Optical spectroscopy is also a method of qualitative analysis: For instance, the fluorescence spectrum of Eu^{3+} in $LaAlO_3$ is well known (*8*) and allows this compound to be identified in a phase mixture.

I. Preparation of Samples and Analysis

Two types of synthesis were attempted: the fusion in a solar furnace and the solid phase reaction of the oxide mixture. We established that the samples quenched from the melt always exhibit two or three phases, depending on the initial composition, whereas by solid-state reaction it was possible to obtain diphasic and monophasic samples. This result is significant since it enabled us to define the exact composition of the β phase and to obtain its fluorescence spectrum. Indeed, we noticed that the optically active Eu^{3+} ions present in a $\beta + P$ mixture occupy preferentially the La^{3+} sites in the perovskite (so that they completely hide the presence of the β phase for fluorescence study).

Our samples were obtained by physical mixture of the oxides (about 2 g) pressed in thin plates of 0.7 × 7 cm at 500 kg/cm^2, then fired in a lime-stabilized zirconia heating element operating at 1750–1860°C during 24–48 hr in oxidizing atmosphere (*9*).

The X-ray diffraction pattern of β(La), very similar to that of β(Na), is very easy to identify. According to the initial composition we could detect the phases which are reported in column 3 of Table I. In this table, as in the following, the compositions are given as the ratio: Al_2O_3/Ln_2O_3. From X-ray results, a pure β(La) phase seems to correspond to a defined compound $12.2Al_2O_3/1Ln_2O_3$ (sample *c*). We shall see that it is not quite true. In sample *b*, subjected to a special high and long heat treatment (1850–1900°C for 70 hr), a circular, high density translucent zone appeared surrounded by a narrow porous zone. From X-ray diffraction and fluorescence analysis, these two zones could be identified as β(La) and $LaAlO_3$ (perovskite), respectively. Samples *c* and *b* "translucent" have the same fluorescence spectrum, which will be discussed in detail in Section II and referred to as spectrum of type 1.

Samples *d*, *e*, *f* produce X-ray diffraction patterns similar to those of *c* and *b* "translucent" (with the exception of additional lines attributed to α-Al_2O_3), whereas they give different fluorescence spectra. These spectra exhibit a continuous evolution until the appearance denoted by type 2.

The Castaing microprobe analysis of the percentage of Al, La, and Eu in samples *b*,

TABLE I.
Identified phases with respect to sample composition

Sample	Initial Composition	X-Ray Identified phases	Fluorescence Identified phases
a	9.25/1	P ($LaAlO_3$) + β	P
b	10.60/1	P + β	P + β(type 1)
c	12.20/1	β	β(type 1)
d	13.80/1	β + α(Al_2O_3)	Continuous evolution
e	16.90/1	β + α	
f	25.20/1	β + α	β(type 2)

c, *e* displays a fairly large range of composition of the pure β(La) phase, the measured limits of which are reported in Fig. 2 (10.3–14.7/1).

The separation in two regions observed in sample *b* is confirmed by analysis. Inclusions of composition $LaAlO_3$ are to be seen within the narrow porous band. However, inclusions of a size below the limit of sensibility of the microprobe (1 μm^2) are likely to occur even in the translucent zone. The error caused by these inclusions explains that the experimental lowest value of Al_2O_3/Ln_2O_3 is smaller than 11/1, which is theoretically impossible, as will be discussed further. In the same way, for higher aluminum content (sample *e*), α-Al_2O_3 inclusions are observed. It is highly probable that small unobserved inclusions present in sample *e* alter the analysis and make the apparent Al_2O_3 content in β(Al) too high. The real existence range of the β phase will then be reduced in unknown proportions but it seems unlikely, with respect to the fluorescence spectra, that the β phase is a well-defined compound.

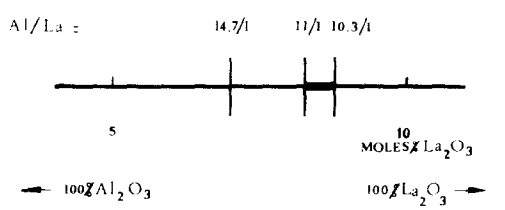

FIG. 2. Composition range of the pure β(La) phase.

II. Spectroscopy

(a) *Experimental Methods*

Fluorescence. The fluorescence spectra are recorded by means of an HRS spectrometer followed by a Hamamatsu R 374 photomultiplier and a synchronous detector. Exciting light at 2500 Å is provided by an OSRAM HBO 150-W lamp equipped with a Wood filter. The spectral range investigated, between 5700 and 6300 Å, includes the $^5D_0 \rightarrow {}^7F_{0,1,2}$ transitions. In the case of a low-point symmetry, these transitions are split into a maximum of one, three, and five lines, respectively. We shall consider later on, several types of highly symmetrical point sites as D_{3h} or less symmetrical as C_s. In the two cases, the theoretical number of lines is for $^5D_0 \rightarrow {}^7F_0$: 0 and 1, and for $^5D_0 \rightarrow {}^7F_2$: 1 and 5, respectively (*10*). In our spectra the $^5D_0 \rightarrow {}^7F_1$ transition is weak and confused; we shall not take it into account for the discussion.

Lifetimes measurements. The $1/e$ lifetime of the emitting level of the rare-earth ion depends on the surroundings of the latter (*11*). Thus we proceeded in lifetime measurements for the main spectral lines of $^5D_0 \rightarrow {}^7F_0$ and $^5D_0 \rightarrow {}^7F_2$ transitions. The light pulses are produced

by a General Radio Strobotac flash lamp and the detection unit is a Schlumberger oscillograph. We notice that the measured lifetimes unfortunately display quite close values. However, by careful inspection, they give some information about the number of different Eu^{3+} sites and corresponding lines in both transitions.

(*b*) *Results*

The fluorescence spectra are presented in Fig. 3 and Table II. Contrary to the observations made on X-ray patterns, the aspect of the fluorescence spectrum changes progressively with the initial composition of the samples. The upper spectrum on Fig. 3 was produced by sample *c* (see Table I), the middle one by sample *d*, and the lower one by *e*.

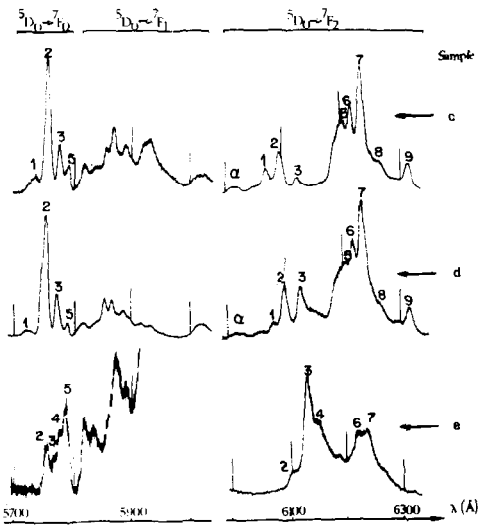

FIG. 3. Fluorescence spectra of β(La) at 300°K.

TABLE II.
Spectroscopical data

Line N°	Transition	Wavelength (Å)	Energy (cm^{-1})	Lifetime τ(ms) $I = I_o e^{-t/\tau}$	
				300K	77K
1	$^5D_0 \rightarrow {}^7F_0$	5720	17482	-	-
2		5748	17397	0.75	0.76
3		5767	17340	1.29	1.38
4		5771	17328	-	-
5		5783	17292	-	1.39
α	$^5D_0 \rightarrow {}^7F_2$	6010 to 6050	16639 to 16529	-	-
1		6065	16488	-	1.23
2		6090	16420	-	1.26
3		6120	16340	1.37	1.66
4		6143	16278	-	-
5		6196	16139	1.25	1.43
6		6212	16098	-	1.00
7		6228	16056	0.85	1.04
8		6255	15987	-	-
9		6310	15848	0.85	0.91

(c) *Comments*

The following information can be derived from the recorded spectra.

The $^5D_0$ level positions. Lines 1, 2, 3, 4, 5 in $^5D_0 \rightarrow {}^7F_0$ imply *the presence of at least five different cristallographic sites for the europium atom in the range of composition under study.* The position of the $^5D_0$ levels in the $4f^6$ configuration energy levels scale depends on the Racah parameter values. Those are different for each site and depend on the europium to ligand distance and on the geometry of the ligand arrangement (*12*). As a matter of fact, the positions of the $^5D_0$ levels recorded here are very high in the nephelauxetic scale for Eu^{3+} compounds. For a large number of compounds (*12*), the $^5D_0$ levels are situated between 17,200 and 17,300 cm^{-1} above the ground $^7F_0$ level. Here the lower level (line 5) is situated at 17,292 cm^{-1} and the higher one (line 1) at 17,482 cm^{-1}. Because of their high energy position, there is no doubt that the observed fluorescence lines are $^5D_0 \rightarrow {}^7F_0$ transitions. (On the contrary, if the $^5D_0 \rightarrow {}^7F_0$ line is on the low energy side of the nephelauxetic scale, there is always the problem of confusion with a $^5D_0 \rightarrow {}^7F_1$ transition.)

The high energy values for the $^5D_0$ level may be the indication that the europium to ligand distances are quite large (because in most cases the $^5D_0$ level position is lowered if the distance decreases). However, a high energy position also can be due to a larger decrease of the E_2 and E_3 Racah's parameters versus the E_1 parameter for some geometrical arrangements of ligands. In other words, it can be due to a larger decrease of the F^2 Slater integral versus F^4 and F^6 decreases with respect to the free ion values. This is the case for the Eu^{3+} site in perovskites structures (*12*).

It should also be noted that the $^5D_0 \rightarrow {}^7F_0$ transitions exhibit very strong, sharp lines. This implies that the europium ion is located in quite well-defined sites, displaying only some minor variations in distance or geometry. If the sites were not quite distinct we should observe a broad band spreading over the wavelength range between 5700 and 5800 Å.

The $^7F_2$ crystal field splittings. The $^7F_2$ levels barycenter position with respect to $^7F_0$ depends on the value of the spin–orbit coupling constant, which does not vary very much from compound to compound. As a matter of fact, the barycenter is always located in a rather narrow energy range, for instance: in EuF_3, 1059 cm^{-1} (*13*); Eu in Y_2O_2S, 1033 cm^{-1} (*14*); $Eu(C_2H_5SO_4)_3$, $9H_2O$, 1058 cm^{-1} (*15*), Eu in $LaCl_3$, 1037 cm^{-1} (*16*); Eu in La_2O_3, 1047 cm^{-1} (*17*); Eu in Lu_2O_3, 1061 cm^{-1} (*18*); Eu in KY_3F_{10}, 1041 cm^{-1} (*19*); Eu in $LaAlO_3$, 1021 cm^{-1} (*8*); $EuScO_3$, 1065 cm^{-1} (*20*); EuOF, 1044 cm^{-1} (*21*).

This observation relative to the $^7F_2$ barycenter, together with the observation of enhancement or weakening of spectral lines with composition and lifetime measurements, enable us to find the position of some $^7F_2$ Stark levels with respect to the unsplit $^7F_0$ ground state.

This analysis leads us to the following associations.

I. Line 2 in $^5D_0 \rightarrow {}^7F_0$ as well as 7 and 9 in $^5D_0 \rightarrow {}^7F_2$ should be associated. All of these lines weaken as the alumina content in the sample increases and their lifetime is about 0.9 msec. Moreover, since the $^7F_2$ barycenter must be located near 1050 cm^{-1}, these lines also must be associated with two lines of the weak unresolved group α.

II. Line 3 in $^5D_0 \rightarrow {}^7F_0$ and 1, 2, 6, 8 in $^5D_0 \rightarrow {}^7F_2$ behave in the same way as the former but their lifetime is somewhat higher: 1.30 msec.

III. Line 5 in $^5D_0 \rightarrow {}^7F_2$ may be associated with one or two weak lines in the group of lines α. We have not selected the corresponding $^5D_0 \rightarrow {}^7F_0$ line; it does not seem to be 1, which is too low in the nephelauxetic scale.

IV and **V.** Lines 4 and 5 in $^5D_0 \rightarrow {}^7F_0$, as well as 3 and 4 in $^5D_0 \rightarrow {}^7F_2$ are enhanced when the alumina content increases. We cannot find more accurately how these lines are coupled.

The fluorescence spectra are complex and we cannot avoid the presence of unresolved lines. However, they are consistent with the following assumptions. The last three groups of lines above may be due to D_{3h} point sites. Indeed, for each one of them, one strong line is observed in the $^5D_0 \rightarrow {}^7F_2$ transition, possibly accompanied by one or two weak theoretically

forbidden lines, due to a slight distortion of the site symmetry.

On the other hand, the two first groups cannot be produced by a high symmetry site but rather by Eu^{3+} in a C_s or C_{2v} point site for instance.

III. X-Ray Patterns

(*a*) *Interplanar Spacings*

X-ray diffraction patterns were recorded with a Guinier–de Wolff camera using Cu$K\alpha$ radiation and α-quartz as internal standard.

Table III lists the observed values of d_{hkl}. The refined parameters of the hexagonal unit cell are: $a = 5.560 \pm 0.003$ Å, $c = 22.001 \pm 0.003$ Å.

The observed extinctions agree well with the $P6_3/mmc$ space group. It is important to point out that no change is observed in lattice parameters with respect to the initial content of the sample.

(*b*) *Intensity Measurements*

X-ray intensity measurements were recorded on powder patterns. Since grinding is likely to promote preferred orientations, a small amount of the powder used for intensity measurements was spread on an electron microscope grid and a series of single-crystal diffraction patterns was performed. In this way, we stated no preferred orientation of the grains since, on the whole, all the spots relative

TABLE III.

Observed and calculated interplanar spacings and observed relative intensities for pure β(La)

β alumina (La) a = 5.560 Å c = 22.001 Å			
d obs. (Å)	d calc. (Å)	h k l	I/Io obs.
11.10	11.00	00.2	30
4.71	4.704	10.1	30
4.41	4.411	10.2	20
4.01	4.025	10.3	5
3.68	3.667	00.6	12
3.62	3.623	10.4	10
3.25	3.248	10.5	5
2.773	2.780	11.0	49
2.753	2.750	11.2	20
2.633	2.632	10.7	95
2.482	2.481	11.4	100
2.402	2.407	20.0	< 5
2.285	2.287	20.3	30
2.202	2.200 2.205	00.10 20.4	20
2.182	2.180	10.9	< 5
2.112	2.112	20.5	60
2.010	2.012	20.6	40
1.847	1.847	10.11	11
1.601	1.605 1.601	30.0 30.1	10
1.573	1.575 1.571	21.7 00.14	10
1.389	1.390	22.0	71
1.345	1.347 1.342	22.4 30.9	< 5
1.237	1.241	22.8	< 5
1.230	1.232 1.229	11.16 31.7	< 5

to allowed (*hkl*) planes appeared without any significant preference.

The intensity of the diffraction lines on the Guinier pattern is recorded by means of a microdensitometer (Joyce–Loebl MK III CS) by graphical measurement of the line surface (height × half – value width), planimetry, and numerical output followed by a surface integration. The results in Table III have been averaged from the relative intensities obtained by these different methods.

Under these measurement conditions, no significant variation of the relative intensities as a function of the phase composition is found. The values of the observed factors, F_o, are deduced from that of the relative intensities after correction for the sample film distance, Lorentz polarization factors and multiplicity of the (*hkl*) planes. We used two computer programs for the interpretation of the observed intensities: a program of simulation of the intensities based on a given hypothesis (*22*); and a program of refinement of the F_o by minimizing $\Delta^2 = (F_o - F)^2$ (*23*).

The atomic scattering factors used are directly taken from the tables (*24*) or extrapolated from atoms or ions with the same number of electrons. By Ln^{3+} we mean the totality of the lanthanide ions present (La^{3+} + Eu^{3+}). But the atomic scattering factors used are those of La^{3+}.

(*c*) *X-Ray Calculations*

The structure determination was made step by step by means of simple intensity calculations based on a priori assumptions at first, then by refinement of two or three parameters at a time when we believed we were near the solution. As it is, we think it represents nearly quantitatively the mirror plane structure, and this is supported by the comparisons we shall make later on with β(Na), β(Ag), and magnetoplumbite mirror plane structures.

In view of the very small variations in atomic positions found by different authors within the spinel blocks, the number of lines detected is not sufficient to allow us to reconsider the structure of these blocks. We make the assumption that the β(La) spinel blocks are identical to those of β(Na) described by Wyckoff (*4*). Besides, the possibility of a nonstoichiometry due to the mixture of two phases β ($c \cong 22$ Å) and β″ ($c \cong 33$ Å) as was shown by Bevan *et al.* (*25*) in β(Na) samples was ruled out. Indeed, we can see in Fig. 4 a regular sequence of metallic planes every 11 Å over a distance of 1000 Å at least for our β(La) samples. The high-resolution microscopy image was obtained with a Jeol, JEM 100C microscope.

As a first step we have assumed that the mirror plane has the exact formula $[LnO_2]^-$

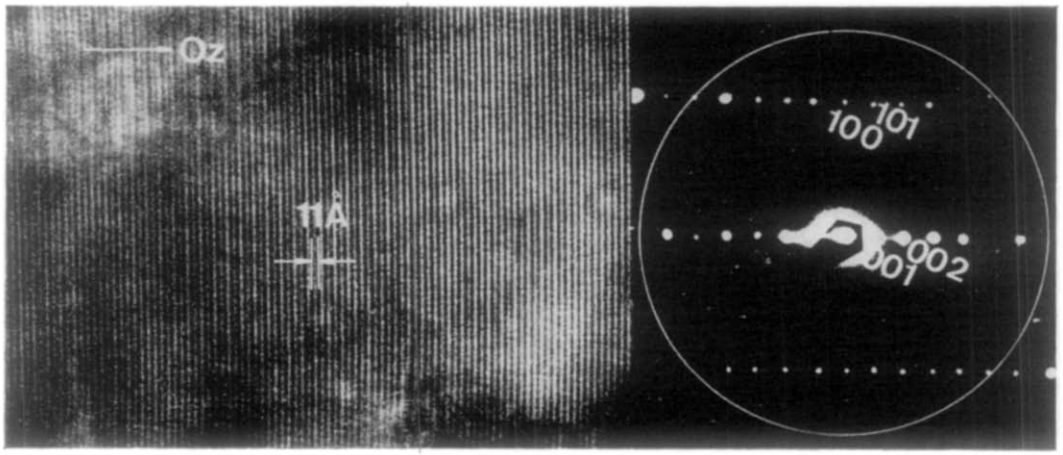

FIG. 4. Imaging of (002) planes in β(La).

which takes into account the electrical neutrality. The three simplest hypotheses which, in fact, amount to displacing the same pattern in the mirror plane, are:

(1)	*Ln* in (2*b*)	O in (2*c*) and (2*d*)	$R = \|\|F_o\| - \|F\|\|/\|F_o\| = 25\%$
(2)	*Ln* in (2*c*)	O in (2*b*) and (2*d*)	$R = 40\%$
(3)	*Ln* in (2*d*)	O in (2*b*) and (2*c*)	$R = 15\%$

Hypotheses (2) and (3) seem a priori rather unprobable, because of the presence of oxygen atoms in (2*b*) located at 2.33 Å between two oxygens (4*e*).

Intensity calculations based on these three possibilities show, however, that experimental data are best represented by the third assumption ($R = 15\%$). This is highly significant as far as location of *the major part of lanthanum atoms* in the unit cell is concerned. It means that nearly all Ln^{3+} are located at the (2*d*) position, or quite near it.

By varying the occupation factor of *Ln* (2*d*), *R* falls from 15 to 11% (for *f* [*Ln* (2d)] = 0.77, i.e., 1.55 *Ln* (2*d*) per unit cell).

Another forward step is made by locating oxygens in (6*h*) ($x = \frac{1}{6}$) sites, and this allows the reliability factor to drop to 8% (Table IV.1).

Obviously, this distribution results in an excessive amount of oxygen in the mirror plane and the nature of the atoms present within it must be discussed. In particular, it has been noticed above that the (2*b*) site is not suitable for oxygen atoms, but this site may be occupied by a cation, i.e., by Ln^{3+} or, as will be seen later, by Al^{3+}. Therefore, we have carried out refinements with this new hypothesis and have obtained the two sets of values (Tables IV.2 and IV.3) for which *R* is at a minimum (7.8%).

At this stage we could not improve *R* any more in a significant manner. However, it was suggested to us that a certain amount of lanthanum atoms could be located in a (6*h*) position near (2*d*) and not exactly in it. A refinement carried out with the *x* variable near (2*d*) ($x \cong 0.67$) leads to a minimum *R* factor of 7.5% for $x = 0.71$ (Tables IV.4 and IV.5). Finally, the information given by the intensity calculations is the following:

The major part of Ln^{3+} is located *in* or *in the vicinity of* (2*d*) (the so-called "B.R." position in the literature). Indeed, the filling up of (2*d*) positions by another sort of atom could never give a satisfactory result in view of the enormous difference between atomic scattering factors of Ln^{3+} on one side and O^{2-} or Al^{3+} on the other side (F_{diff} (Ln^{3+})/F_{diff} (Al^{3+} or O^{2-}) ~ 5).

The other conclusions we shall draw are only tentative:

Oxygens occupy (2*c*) and (6*h*) ($x = \frac{1}{6}$) sites, which are obviously anionic sites.

TABLES IV AND V.

Results of X-ray intensity refinement calculations with respect to site occupancy in the mirror plane

Calc.	2d(2/3 1/3 1/4)			2b(0 0 1/4)			6h(0.71 0.29 1/4)			2c(1/3 2/3 1/4)			6h(1/6 5/6 1/4)			R
	ion	f	n	ion	f	n	ion	f	n	ion	f	n	ion	f	n	
1	Ln	0.77	1.55	O	(1.12)	(2.24)				O	0.60	1.20	O	0.56	3.38	8.0 %
2	Ln	0.77	1.55	Ln	0.15	0.30				O	0.60	1.20	O	0.56	3.38	7.8 %
3	Ln	0.77	1.55	Al	0.80	1.60				O	0.60	1.20	O	0.56	3.38	7.8 %
4	Ln	0.37	0.74	Ln	0.16	0.32	Ln	0.13	0.78	O	0.59	1.18	O	0.48	2.88	7.5 %
5	Ln	0.37	0.74	Al	0.85	1.68	Ln	0.13	0.78	O	0.58	1.16	O	0.48	2.88	7.5 %

f=occupancy factor — n=number of atoms per unit cell : number of equipoints x occ. factor — $R = \Sigma\,||Fo| - |F||\,/\,\Sigma|Fo|$

The (2*b*) position is occupied by a cation, Ln^{3+} or Al^{3+}.

These conclusions relative to the location of cations in the mirror plane are confirmed by comparison with single-crystal data of β(Na), β(Ag), and magnetoplumbite (Fig. 1). If there are cations in the so-called "m.O." position (6*h*) ($x = \frac{5}{6}$), it is in a low proportion, which cannot be detected with our powder data. As in β(Ag) and magnetoplumbite structures, in β(La) some cations are located in (2*b*), the "a.B.R." position.

IV. Discussion

If we associate information given by both X-rays and optical study, we can make further comments on the structure. We have pointed out the complete insensibility of X-ray line intensities on the phase composition of β(La). All the X-ray calculations give a high occupancy factor for *Ln* (2*d*), which cannot be replaced by something else. So we believe that the whole range of compositions of β(La) is ruled by the nature of the (2*b*) cations.

Our structural hypotheses are:

For high lanthanum contents, the (2*b*) position is occupied by Ln^{3+}. This occupation of the mirror plane will be referred to as of "β-type." The (2*b*)–(2*d*) = 3.20 Å and the (6*h*) ($x = 0.71$)–(2*b*) = 2.80 Å distances are much lower than the La–La distance in the metal (3.80 Å). Thus, a simultaneous occupation by Ln^{3+} of (2*b*) and (2*d*) or (6*h*) ($x = 0.71$) is unacceptable and the maximum number of lanthanum per unit cell is 2, the corresponding limit composition is 11/1. If Ln^{3+} is located in (2*b*), the (6*h*) ($x = \frac{1}{6}$) cannot be occupied and neighbor oxygens are in (2*c*). The point site in this ideal position is D_{3h}; the coordination number $C_N = 5$ (Fig. 5a). The *Ln*–O (2*c*) distances in the mirror plane are 3.20 Å which are large, but above and beneath the lanthanide ion are located two oxygens (4*e*) at 2.33 Å. This small distance may induce a slight displacement of Ln^{3+} in the mirror plane and a distortion of the site.

If the (2*b*) position is empty (which is realized for about three-fourths of the unit cells) and if oxygens are located in or near (2*c*), then the Ln^{3+} (2*d*) can be removed easily from this position in (6*h*) ($x = 0.71$). The point site around Ln^{3+} is then of the C_s type. Our spectroscopical data display two fairly well defined C_s type point sites, which could be associated for instance with two values for *x* (6*h*), but this has not been shown by X-ray calculations. The *Ln*–O (2*c*) distances in the mirror plane = 3.62 and 2.95 Å and Ln–O (12*k*) = 3.08 and 2.72 Å are large and agree

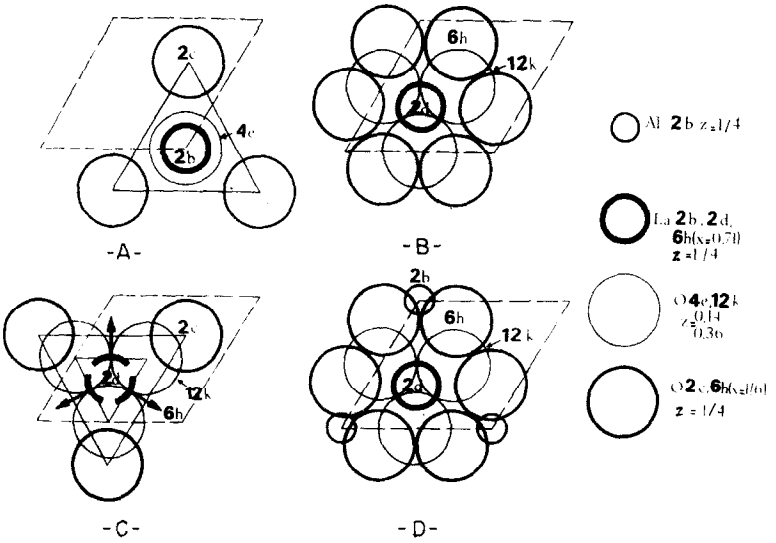

FIG. 5. Ln^{3+} point sites in β(La).

TABLE V

Calc.	2d(2/3 1/3 1/4)			2b(0 0 1/4)			6h(0.71 0.29 1/4)			2c(1/3 2/3 1/4)			6h(1/6 5/6 1/4)			R
	ion	f	n	ion	f	n	ion	f	n	ion	f	n	ion	f	n	
1	Ln	0.77	1.55	Ln	0.15	0.30	Ln	0.02	0.12	O	0.62	1.24	O	0.57	3.41	7.8 %
2	Ln	0.66	1.32	Ln	0.16	0.32	Ln	0.04	0.24	O	0.60	1.20	O	0.54	3.24	7.4 %
3	Ln	0.54	1.08	Ln	0.16	0.32	Ln	0.08	0.48	O	0.60	1.20	O	0.51	3.06	7.3 %
4	Ln	0.24	0.48	Ln	0.17	0.34	Ln	0.17	1.02	O	0.58	1.16	O	0.44	2.64	7.7 %

f=occupancy factor – n=number of atoms per unit cell : number of equipoints x occ. factor $-R = \Sigma \, ||Fo|-|F|| \, / \Sigma |Fo|$

with the $^5D_0$ level experimental position (line 2 or 3), which is high in the nephelauxetic scale (see section II.c) $C_N = 12$ (Fig. 5c). Note that under this hypothesis the oxygen atoms are probably removed from the true (2*c*) position.

If oxygens are located in (6*h*) ($x = \frac{1}{6}$), Ln^{3+} will more likely occupy the true (2*d*) position. The corresponding point site is D_{3h}·*d* [*Ln*–O (6*h*)] = 2.77 Å and *d* [*Ln*–O (12*k*)] = 2.83 Å, $C_N = 12$ (Fig. 5*b*).

To summarize, the mirror plane structure of "β-type" promote nonsymmetrical C_s (or distorted D_{3h}) environments for Ln^{3+} and quite large lanthanide to ligand distances (all but one). This is rather consistent with the I, II, and III groups of fluorescence lines (Section II), which vanish as the lanthanum content decreases.

For high aluminium contents, Al^{3+} is located in (2*b*). The O^{2-} content of the mirror plane must be higher and more likely of the (6*h*) ($x = \frac{1}{6}$) type. Note that the total occupation of oxygen (6*h*) ($x = \frac{1}{6}$) site leads to a theoretical boundary formula $[Ln_{5/6}\,Al_{5/6}\,O_3]^-$ for the mirror plane, i.e., an overall limit composition of 14.2/1. This mirror plane structure of "magnetoplumbite type" is characterized by a highly symmetrical D_{3h} point site for Ln^{3+} (Fig. 5d). The mirror plane occupation is more dense and the *Ln*–O distances are short: *d*[*Ln*–O (12*k*)] = 2.83 Å and *d*[*Ln*–O (6*h*)] = 2.77 Å, $C_N = 12$.

The magnetoplumbite type mirror plane structure promotes a symmetrical environment for Ln^{3+} and shorter *Ln*–O distances. This is consistent with the groups of fluorescence lines denoted by IV and V in Section II.

At this stage we have carried out a series of calculations. The *f* [*Ln* (2*d*)] being fixed at different values, the other occupation factors are allowed to move. When *f* [*Ln* (2*d*)] decreases (which, in our hypothesis, means that the proportion of magnetoplumbite type diminishes), *f* [*Ln* (6*h*) ($x = 0.71$)] increases, and the *R* value is only slightly modified (Table V). Moreover, *f* [O (2*c*)] + *f* [O (6*h*) ($x = \frac{1}{6}$)] decreases, which is consistent with the hypothesis of a lower cationic content in the unit cell.

In Table V, the stoichiometry is not maintained but one has to keep in mind that our samples are in fact mixtures of several compounds in various proportions. In particular, "*Ln* (2*b*)" must be understood as: *y Ln* (2*b*) + *z*Al (2*b*) with unknown *y* and *z*.

The complete solution is undoubtedly more complex than the description we have attempted. For instance, we cannot ascribe a precise environment to each set of spectral lines. Other point sites, which have not been considered, may exist.

It is simply noteworthy that fluorescence data are rather consistent with the hypothesis of quite well-defined point sites; the structural meaning of this is the juxtaposition of small ordered domains. It is not possible at this stage to detail more features of the different domains and a fortiori the linking of domains together.

Conclusion

To conclude, the phase referred to by other authors as β-alumina (La) would be, in

fact, a structural intermediate between the β-aluminas of monovalent ions ("$AgAl_{11}O_{17}$" for instance), and the complex aluminates of divalent ions ($BaAl_{12}O_{19}$), of magnetoplumbite type. Some authors (*26*) succeeded in partially substituting La^{3+} for Ba^{2+} in this last set of compounds. The microprobe analysis and structural considerations lead us to suggest a range of compositions lying between $11Al_2O_3/1Ln_2O_3$ and $14Al_2O_3/1Ln_2O_3$.

The structural problem of the so-called β(La) phase is complex and the absence of single-crystal data has until now inhibited complete resolution of this structure. However, we obtained many interesting results from our polycrystalline sample. The β(La) phase is characterized by spinel blocks on both sides of a mirror plane, the nature and structure of which may vary significantly within the theoretical limits:

$$[LaO_2]^- \quad \text{and} \quad [La_{5/6}\square_{1/6}Al_{5/6}\square_{1/6}O_3]^-$$

A high percentage of Ln^{3+} is always found to be in or near the (2*d*) sites. The nature and degree of occupancy of the (2*b*) site are sufficient to cover the observed range of composition, in agreement with the measured X-ray intensities. If this site is occupied by lanthanide ions the mirror plane structure approaches that of β(Ag). If Al^{3+} ions are located in (2*b*), the mirror plane is approximate to that of magnetoplumbite. The oxygen atomic scattering factor is too low to allow accurate indications about anions, which may, however, be located in (2*c*) and (6*h*) ($x = \frac{1}{6}$).

Although powder X-ray diffraction patterns do not vary between boundary compositions of the β(La) phase, it is highly probable that we are always dealing with a mixture of two or several "compounds" in various proportion. This last assumption is supported by the progressive modification of fluorescence spectra with the sample composition. This work shows the value of using statistical (as X-ray diffraction) and local (spectroscopical results) investigations together.

Acknowledgments

The authors are greatly indebted to Mr. C. Bahezre who performed the Castaing microprobe analysis on the lanthanum β alumina samples. The high-resolution microscopy images and diffraction patterns were obtained by Dr. G. Schiffmacher. Dr. J. P. Coutures furnished us with several samples which had been melted in the Odeillo solar furnace.

References

1. R. S. ROTH AND S. HASKO, *J. Amer. Ceram. Soc.* **41**, 4, 146 (1958).
2. M. ROLLIN AND P. H. THAN, *Rev. Int. Hautes Temper.* **2**, 784 (1965).
3. D. GOLDBERG, *Rev. Int. Hautes Temper. Refract.* **5**, 181 (1968).
4. R. W. G. WYCKOFF, "Crystal Structures," p. 496, Interscience, New York (1948).
5. F. S. GALASSO, "Structure and Properties of Inorganic Solids," Pergamon Press, New York (1970).
6. G. R. PETERS, M. BETTMAN, J. W. MOORE, AND M. D. GLICK, *Acta Crystallogr.* **B27**, 1826 (1971).
7. W. L. ROTH, *J. Solid State Chem.* **4**, 60 1972).
8. M. FAUCHER AND P. CARO, *J. Chem. Phys.* **63**, 446 (1975).
9. M. FAUCHER, K. DEMBINSKI, AND A. M. ANTHONY, *Amer. Ceram. Soc. Bull.* **49**, 707 (1970).
10. J. L. PRATHER, "Atomic Energy Levels in Crystals," U.S. Department of Commerce N.B.S. 19 p. 58 (1961).
11. H. FOREST AND G. BAN, *J. Electrochem. Soc.* **116**, 4, 474 (1969).
12. P. CARO, O. BEAURY, AND E. ANTIC, *J. Physique*, in press.
13. H. H. CASPERS, H. E. REST, AND J. L. FRY, *J. Chem. Phys.* **47**, 4505 (1967).
14. O. J. SOVERS, *J. Chem. Phys.* **51**, 5330 (1969).
15. E. V. SAYRE AND S. FREED, *J. Chem. Phys.* **24**, 6, 1213 (1956).
16. L. G. DE SHAZER AND G. H. DIEKE, *J. Chem. Phys.* **38**, 9, 2190 (1963).
17. C. LINARES AND F. GAUME-MAHN, *C.R. Acad. Sci.* **277** (1973).
18. C. LINARES AND F. GAUME-MAHN, *C.R. Acad. Sci.* **265** (1967).
19. P. PORCHER AND P. CARO *J. Chem. Phys.*, in press.
20. M. FAUCHER AND P. CARO, *Mat. Res. Bull.* **10** 1 (1975).
21. L. BEAURY, Thèse de 3éme Cycle, Orsay, France (1972).

22. K. YVON, W. JEITSCKO, AND E. PARTHE, "A FORTRAN IV Program for the Intensity Calculation of Powder Patterns," University of Pennsylvania (1969).
23. W. R. BUSING, K. O. MARTIN, AND H. A. LEVY, "A FORTRAN Crystallographic Least Squares Program," Oak Ridge National Laboratory (1962).
24. "International Tables for X-Ray Crystallography," The Kynoch Press, Birmingham, England.
25. D. J. M. BEVAN, B. HUDSON, AND P. T. MOSELEY, *Mat. Res. Bull.* **9**, 1073 (1974).
26. A. DESCHAMPS AND F. BERTAUT, *C.R. Acad. Sci. Paris* **244**, 3069 (1954).